

# Spectral estimator effects on accuracy of speed-over-ground radar

Khairul Khaizi Mohd Shariff<sup>1</sup>, Suraya Zainuddin<sup>2</sup>, Noor Hafizah Abdul Aziz<sup>3</sup>,  
Nur Emileen Abd Rashid<sup>1</sup>, Nor Ayu Zalina Zakaria<sup>2</sup>

<sup>1</sup>Microwave Research Institute, Universiti Teknologi MARA, Shah Alam, Malaysia

<sup>2</sup>Faculty of Electrical and Electronic Engineering Technology, Universiti Teknikal Malaysia Melaka, Hang Tuah Jaya, Malaysia

<sup>3</sup>Faculty of Electrical Engineering, Universiti Teknologi MARA, Shah Alam, Malaysia

## Article Info

### Article history:

Received Jul 21, 2021

Revised Apr 8, 2022

Accepted Apr 18, 2022

### Keywords:

Accuracy evaluation

Autoregressive

Burg algorithm

Spectral processing

Speed-over-ground radar

## ABSTRACT

Spectral estimation is a critical signal processing step in speed-over-ground (SoG) radar. It is argued that, for accurate speed estimation, spectral estimation should use low bias and variance estimator. However, there is no evaluation on spectral estimation techniques in terms of estimating mean Doppler frequency to date. In this paper, we evaluate two common spectral estimation techniques, namely periodogram based on Fourier transformation and the autoregressive (AR) based on burg algorithm. These spectral estimators are evaluated in terms of their bias and variance in estimating a mean frequency. For this purpose, the spectral estimators are evaluated with different Doppler signals that varied in mean frequency and signal-to-noise ratio (SNR). Results in this study indicates that the periodogram method performs well in most of the tests while the AR method did not perform as well as these but offered a slight improvement over the periodogram in terms of variance.

*This is an open access article under the [CC BY-SA](https://creativecommons.org/licenses/by-sa/4.0/) license.*



## Corresponding Author:

Khairul Khaizi Mohd Shariff

Microwave Research Institute, Universiti Teknologi MARA

Shah Alam, Malaysia

Email: khairulkhaizi@uitm.edu.my

## 1. INTRODUCTION

Recently, speed-over-ground (SoG) radar has attracted attention as a technique to estimate vehicle speed through contactless measurements [1]–[4]. Unlike the conventional wheel speed sensor, SoG radar can deliver true ground speed because its estimate is independent of wheel conditions such as slipping and locking. It is expected that SoG radar will become more prevalent in the future, owing to the increase in demand for true ground speed measurement for vehicle safety systems such as anti-braking systems (ABS) and electronic stability control (ESC) [5].

SoG radar technique utilizes Doppler frequency to estimate the vehicle speed. There are several studies based on spectral estimations [6], [7], with the most popular method is based on the fast Fourier transform (FFT) because it has low computational complexity and is easy to use. This method is based on the decomposing sinusoidal component of the Doppler signal whose phase and amplitude vary across frequencies. Several approaches can be used to compute the FFT power spectrum, some of the methods that have been evaluated for SoG radar are periodogram [8] and Welch's method [9]. Nevertheless, the FFT-based method has a critical issue with SoG radar. In practice, the Doppler frequency is non-stationary and can change rapidly according to vehicle motions, but FFT requires the frequency within the analysis window to be stationary. To adapt to the rapid change of Doppler frequency, the analysis window is fixed to

a short length, with a typical duration of fewer than 100 milliseconds. However, such a short length produces poor spectral resolution which consequently affects the accuracy of SoG speed measurement.

Spectral estimation based on the autoregressive (AR) model has also been evaluated for SoG radar. The choice of using the AR method is largely motivated by improved frequency resolution for short data length [10]. Unlike the FFT approach, this method models the data outside the processing length, which improves the spectral resolution of the observed signal [11]. AR spectrum can be computed using several techniques including the Yule-Walker and Burg algorithm [12]. However, the main disadvantage of the AR method is that they are more computationally intensive compared to FFT and incorrect modeling of the signal may lead to statistical instability of spectra.

This paper investigates the performance of SoG radar designed based on two spectral estimators namely periodogram which is based on Fourier transformation and Burg algorithm which is based on AR method. For this purpose, the theoretical aspects of both Fourier transformation and AR were reviewed. A simulation approach is used to test the spectral estimator and to provide comparative data of performance. Finally, graphical plots and tables are used to explain the performance of each estimator. The remainder of this article is arranged in the following manner. The signal processing formulation and methodology are presented in section 2. The simulation procedure is presented in section 3. The results and their performance analysis are presented in section 4 and finally, section 5 concludes the work on this paper.

The assessment of spectral estimator performance for SoG radar requires an understanding of the processes underlying the generation of Doppler signal spectrum, referred here as ‘‘Doppler spectrum’’. Consider a SoG setup illustrated on the top part of Figure 1. A radar with an antenna beamwidth of  $\theta$  is mounted on a vehicle and faced the ground surface at an angle of  $\alpha$  to the direction of the moving vehicle with a velocity of  $v$ . The propagation of waves emitted from the radar to the moving ground surface eventually backscattered toward the radar. Accordingly, Doppler shift from each scatterer on the ground is accumulated in the radar as the vehicle moves longitudinally above the ground. The resultant spectrum has peak magnitude when the antenna boresight beams directly to the moving ground and the magnitude reduces as it goes away from the boresight.

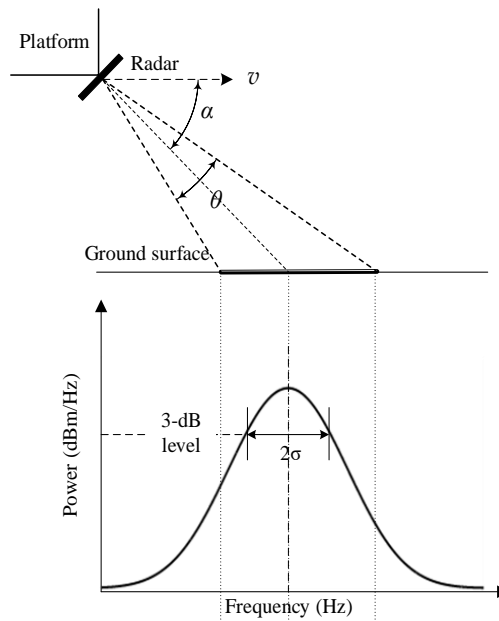


Figure 1. The principle of Doppler spectrum generation

The Doppler spectrum of the first half-power arising from that process has a shape that can be approximate by a Gaussian function [7]:

$$G(f) = \frac{1}{\sigma\sqrt{2\pi}} \exp\left[-\frac{(f-f_0)^2}{2\sigma^2}\right] \quad (1)$$

where  $G(f)$  is the spectrum coefficient,  $\sigma$  is the standard deviation, and  $f$  and  $f_0$  is the Doppler frequency, and mean Doppler frequency of the distribution. The standard deviation and the mean frequency of the spectrum

are related to the radar antenna beamwidth and the vehicle speed respectively [13]. The (2) and (3) provide the main characteristics shape of the Doppler spectrum.

$$v = \frac{f_0 \lambda}{2 \cos \alpha} \quad (2)$$

$$\sigma \approx \frac{v}{\lambda} \theta \sin \alpha \quad (3)$$

The location of the mean Doppler frequency is at the peak magnitude of the spectrum. Nonetheless, the actual spectrum found in practice has random amplitudes near the peak of the spectrum [13]. This amplitude fluctuation is due to the random scattering processing of microwaves on the ground surface which randomly modulates the amplitudes of the spectrum [14]. Thus, making detection of mean frequency difficult.

## 2. RESEARCH METHOD

The proposed framework for evaluating the spectral estimators is shown in Figure 2. In this approach, the spectral estimators estimate Doppler spectra provided. Afterward, the mean Doppler frequencies are extracted. Finally, the spectral estimator performances namely bias, standard deviation, and root mean square error (RMSE) are recorded. All numerical simulations are performed in matrix laboratory (MATLAB).

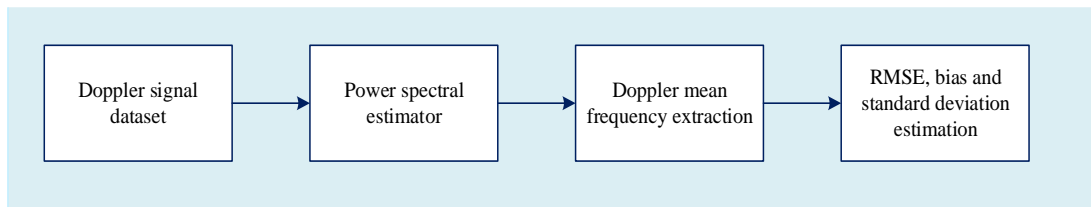


Figure 2. The framework of spectral estimator evaluation

### 2.1. Synthetic Doppler signal and dataset

The simulated signal in this work is generated in the same way as in [15]. Its parameters are: vehicle speed,  $v$  mean Doppler frequency,  $f_m$  radar antenna beamwidth,  $\theta$  radar beam depression angle,  $\alpha$  carrier frequency,  $f_c$  sampling frequency,  $f_s$  and signal-to-noise ratio, SNR. Additionally, the yielded “bell-shape” spectrum such as shown in Figure 1 is incorporated into the model using (2) and (3). All Doppler signal in this study is created using the following radar parameters:  $\alpha=45$  degrees,  $\theta=24$  degrees,  $f_c=24.125$  GHz, and  $f_s=25$  kHz. The antenna radiation pattern is assumed to have a Gaussian pattern at the first half-power.

Doppler signals were generated with a mean Doppler frequency range between 0.1 kHz and 4.0 kHz at 0.1 kHz intervals. For each mean frequency, 500 Doppler signals were generated using the same mean frequency but with randomized white noise. On top of that, Doppler signals were also generated for four levels of SNR values of 20 dB, 30 dB, 40 dB and 50 dB. A total of 80,000 Doppler signals were generated for the evaluation process. It should be pointed out here that the four levels of SNR value (20 to 50 dB) and range of Doppler frequencies selected in this work are based on some states of practical SoG operation found in practice. Table 1 indicates the relationship of SNR, and mean frequencies to some states found in the real world. Figure 3 shows an example of 500 samples of time-series Doppler signal for vehicle speed moving at constant speed  $v=40$  km/h which corresponds to a mean Doppler frequency,  $f_m=1$  kHz, and SNR values of SNR=40 dB. The in-phase and quadrature components of the signal are indicated with a solid and dashed line, respectively.

Table 1. The relationship between test values and actual state conditions

Parameters	Values	State conditions [16]
SNR	20–50 dB	20 dB: Water surface in excited condition 40-50 dB: Dry asphalt surface
Mean Doppler frequency, $f_m$	0.1 to 4.0 kHz	Vehicle speed between 2.9 to 126.7 km/h

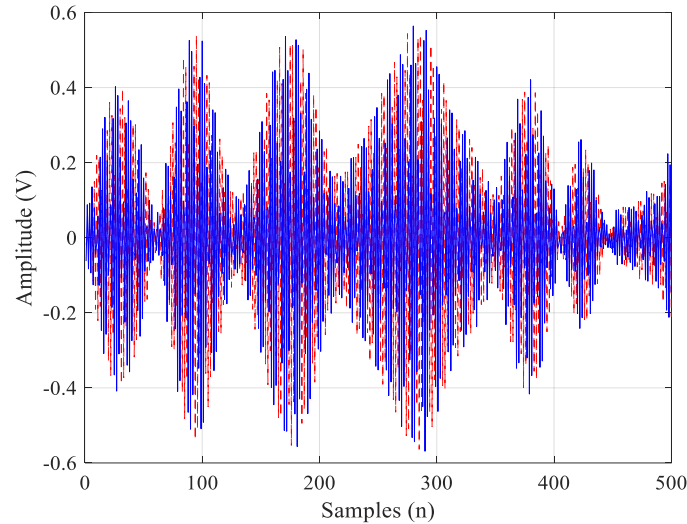


Figure 3. An example of time-series Doppler signal

## 2.1. Power spectral estimator

### 2.1.1. Periodogram

The periodogram of an  $N$  points of discrete Doppler signal,  $x(0), x(1), \dots, x(n-1)$  is given by (4) [17]:

$$P_{pe}(f) = \frac{1}{N} \left| \sum_{n=0}^{N-1} x_n \exp(-j2\pi fn) \right|^2 \quad (4)$$

where  $f$  is the frequency. The sequence of  $x(n)$  is divided into segments of fixed length window, and at the same time, a window function is applied to each segment before the periodogram computation. Typically, fast Fourier transform (FFT) is used for an efficient computation of DFT, in which the signal sequence is divided into frames of  $2^N$  i.e., 256, 518, and 1024. The equivalent frequency resolution is  $1/N$ , for example, the periodogram sample sequence is  $0, 1/N, 2/N \dots (N-1)/N$ . Since the frequency resolution is inversely proportional to the sample length, the precision of frequency measurement is restricted by the frequency resolution. A windowed sinusoid in the time domain produces  $\text{sinc}(x)/x$  function with sidelobes in the transform domain. Depending on the windowing function used, the sidelobes level can have a substantial effect on the effective Doppler signal SNR of the transform.

The number of periodogram frequency samples can be increased by the interpolation process. However, this approach is computationally costly. An efficient approach is to perform zero-padding; a process of which adding zeroes in the discrete Doppler signal before the FFT computation.

$$M = uN, x_{zp} = \begin{cases} x(n) & \text{if } n < N \\ 0 & \text{otherwise} \end{cases} \quad (5)$$

where  $M$  is the length of the zero-padded signal and must satisfy the  $M > N$  requirement. It is worth mentioning that the zero-padding process does not add more information nor increase the spectral resolution but, artificial increases of frequency samples, thus make it appear that the frequency resolution is increased. Nonetheless, the interpolated periodogram samples may help to reduce the bias in the estimation of the peak frequency component.

### 2.1.2. Autoregressive (AR)

For a given Doppler signal  $x(n)$ , the AR method estimates the model of the Doppler signal as an output of a linear system driven by white noise [17].

$$x(n) = -\sum_{k=1}^p a_p(k) x(n-k) + e(n) \quad (6)$$

Where  $a_p$  is the AR coefficient,  $p$  is the AR model order, and  $e(n)$  is the white noise. The AR method produces a higher spectral resolution than the periodogram approach for short records because the PSD is computed from the model of the Doppler signal. Additionally, the AR method can also resolve two close sinusoids if the model is accurate, and the SNR is high.

The procedure of estimating power spectral density (PSD) based on AR consist of two main steps; first the AR parameters are estimated from the sequence of Doppler signal,  $x(n)$ , and secondly, the PSD is computed. There are many methods to estimate the AR parameters such as Yule-Walker and Burg Algorithm. In this paper, we use the Burg algorithm because it produces a stable AR model, and is relatively efficient [18]. The PSD estimated using the Burg algorithm is defined by (7):

$$P_{ar}(f) = \frac{e_p^2}{|1 + \sum_{k=1}^p a_p(k)e^{-j2\pi f k}|^2} \quad (7)$$

where  $e_p$  is the total of the least square error that computed from the sum of the forward prediction error  $f_p$  and backward prediction error  $b_p$ .

$$f_p(n) = x(n) + \sum_{k=1}^p a_p(k) x(n-1) \quad (8)$$

$$b_p(n) = x(n-p) + \sum_{k=1}^p a_p(k) x(n+1) \quad (9)$$

The details on how the Burg algorithm estimates the AR parameters can be found in [19]. The AR model order can be any order as required with the spectrum approximation become increasingly accurate with the increase of order [20], [21]. Nonetheless, the computational cost increases with the increase of model order with the number of computational operations is proportional to  $O(p^2)$  [22] where  $O$  is the operation complexity. Furthermore, high model order increases the variance of the spectrum [23]. A suitable  $p$ -value that can sufficiently exhibit the properties of the signal but is not too large can be determined using the Akaike information criteria (AIC) and it is given by (10):

$$AIC(p) = \frac{2p}{N} + \log(\sigma_a^2) \quad (10)$$

where  $\sigma_a^2$  is the variance of the estimated prediction error of white noise of model order  $p$ .

## 2.2. Mean frequency estimation

We used two methods namely the maximum magnitude of the smoothed spectrum, and the spectral centroid method to estimate the mean frequency from the Doppler spectrum. They were different on the basis that they differ in terms of approach. Firstly, the maximum amplitude is based on selecting the maximum magnitude of a smooth spectrum. To reduce the effect of random magnitude fluctuations about the spectrum peak, the maximum magnitude is selected after the spectrum is average with an average moving filter of  $n=10$ . Secondly, the spectral centroid is based finding the mass center of the spectrum [24].

$$Centroid = \frac{\sum_{n=0}^{N-1} f(n)S(n)}{\sum_{n=0}^{N-1} S(n)} \quad (11)$$

Where  $f(n)$  is the frequency bins and  $S(n)$  the power of the frequency bin. To reduce the effect of spectral noise into the centroid computation, the center-of-mass is determined by selecting the spectrum main lobe frequency components. In this work, the region of the spectrum main lobe of significant SNR is isolated from the rest of the spectral components. The isolation is performed by removing the components that are less than 10 dB from the noise floor.

## 2.2. Accuracy indicators

A comparative assessment of the spectral estimators is made with the use of three statistical performance indicators. They are bias, standard deviation, and root mean square error (RMSE). Mathematically, they are calculated as (12)-(13) [25]. For every estimation of mean frequency from Doppler signal in the dataset, the accuracy of the spectral estimators are measured using a set of core statistical performance indicators namely bias, standard deviation, and root mean square error (RMSE), and they are defined as (12)-(13) [25].

$$Bias = \hat{f} - f_m \quad (12)$$

$$StdDev = \sqrt{\frac{1}{N-1} \sum_{n=0}^{N-1} (f_m(n) - \bar{f})^2} \quad (13)$$

$$RMSE = \sqrt{\frac{1}{N} \sum_{n=0}^{N-1} (f_m(n) - \hat{f}_m)^2} \quad (14)$$

Where  $f_m$  the measured mean frequency,  $\hat{f}_m$  is the true value of mean frequency and  $\bar{f}_m$  is the average mean frequency of  $N$  observations.

### 3. RESULTS AND DISCUSSION

Figure 4 visually indicates the crude accuracy of approximating mean Doppler frequencies as a spectrum peak using the periodogram and AR-Burg method with Figures 4(a)–(l) show different combination of mean frequency and SNR. The spectra for periodogram and AR are presented using solid and dashed lines respectively. The 1st, 2nd and 3rd row of the plot matrix shows the estimation for mean frequency of  $f_m=0.3$  kHz, 2.1 kHz, and 4.0 kHz respectively with the true location is indicated with vertical dashed lines in the plots. The spectra were computed using 2048 samples of Doppler signal sliced using Hanning window. The equivalent period is 80 milliseconds, and the obtained frequency resolution is 12.2 Hz. For the AR method, the model order was computed for orders between 1 and 50 with order  $p=6$  selected for all spectra presentation. As can be seen from the figure, despite the noisy appearance of the periodogram spectra, their peak is discernible even under the random amplitudes. This method is comparatively reliable to retain the shape of the spectrum main lobe across the value of Doppler frequencies and SNR levels which we consider crucial in the context of extracting the mean Doppler frequencies.

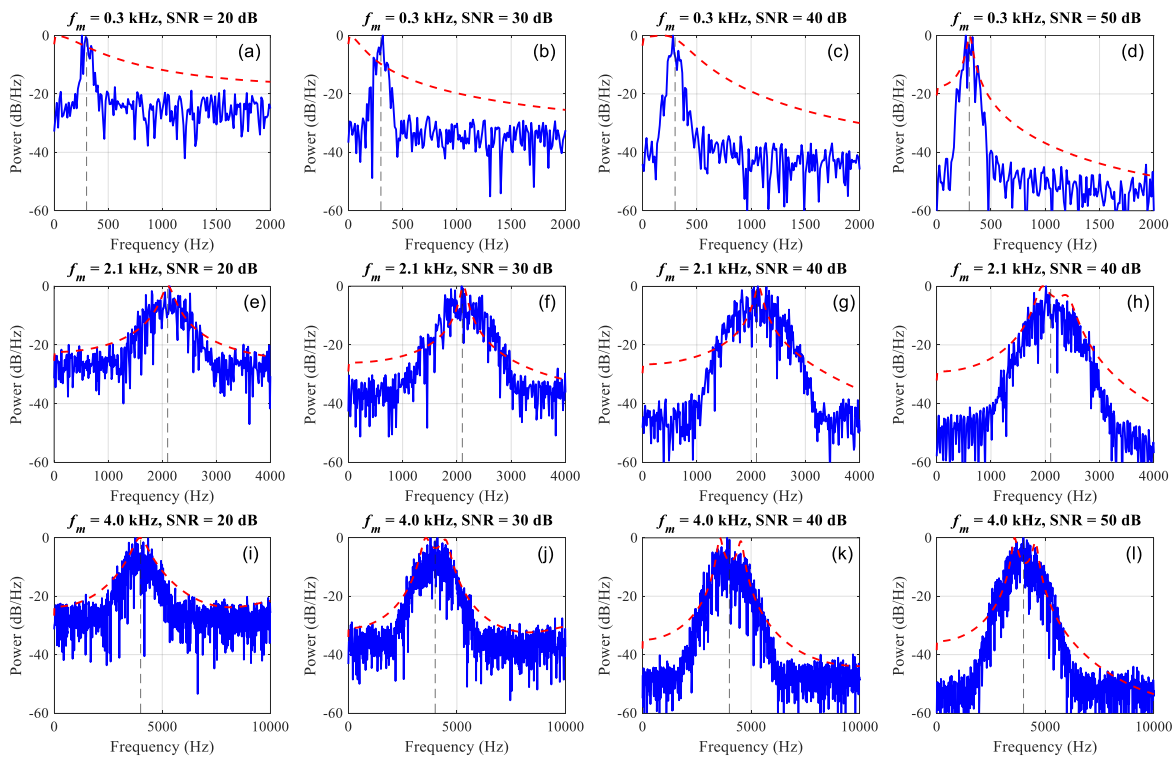


Figure 4. Power spectral density estimated using periodogram and AR Burg algorithm indicated with solid line and dashed line respectively, with (a) to (l) demonstrate various combinations of mean frequency and SNR

On the other hand, for the AR method, the peaks were poorly approximated in some conditions. There were 2 cases in particular; in the first case, the AR method shows a single peak but somewhat shifted to the left from the true mean frequency for location  $f_m=0.3$  kHz and SNR levels between 20 and 40 dB. In the second case, the AR spectra appear to have split peaks for  $f_m=4$  kHz and SNR between 40 and 50 dB. These exhibits indicate the matching capabilities of the AR method to adapt with shape and SNR levels of the Doppler spectrum.

Note that for demonstration in Figure 4, the AR model order for all spectra is fixed at  $p=6$ . However, this value is not an optimal choice for all the Doppler signals in the dataset. We found that for AR method can approximate spectrum with a single peak for order range between  $p=3$  and  $p=30$  with peak become increasingly broader with higher model order. We have shown that for a certain combination of Doppler frequencies and SNR values, the AR spectral approximations were somewhat inaccurate. In these instances, the comparison of the spectral estimation methods is meaningless in terms of performance. Thus, for this reason, we considered some changes in the parameters of spectra would improve the spectrum estimation.

In the case of  $f_m=0.3$  kHz, a simple approach to obtain an AR spectrum with a proper peak is to increase the model order. For example, a reasonably accurate single-peak formation can be obtained for  $f_m=0.3$  kHz and SNR=20 dB using model order  $p=15$ . However, this approach increases the computational cost as discussed in section 2 and therefore is not favorable for the low-cost design of SoG radar system. Instead of increasing the AR model order, we reduced the sampling rate. Our investigation found that a peak can be obtained when we reduced the sampling rate  $f_s=25$  kHz by a factor of 5. However, this approach also reduces the time resolution to 0.41 seconds. For the case of split peaks found on  $f_m=2.1$  kHz and 4 kHz, we keep the same sampling rate, but we reduced the model order to  $p=3$  to obtain a spectrum with single peak. Figures 5(a)–(l) show the AR spectra with different combination of mean frequency and SNR, for  $f_m=0.3$  kHz with new sampling rate,  $f_s=5$  kHz with model order  $p=6$ , and AR spectra for  $f_m=2.1$  kHz and 4 kHz with standard sampling rate but with new model order  $p=3$ .

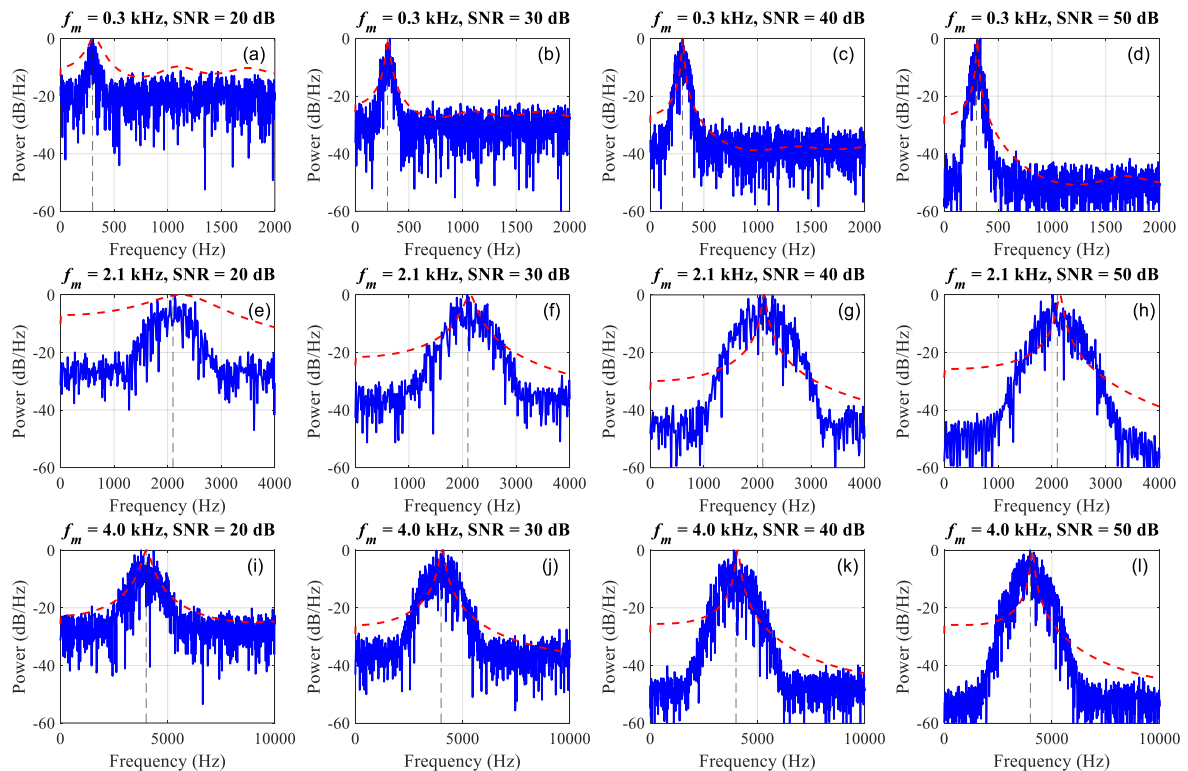


Figure 5. Spectra of periodogram and improved PSD approximation for AR method with (a) to (l) demonstrate various combinations of mean frequency and SNR

The average bias, standard deviation, and RMSE for 500 estimates of mean frequency for  $f_m=0.3$  kHz, 2.1 kHz, and 4 kHz as a function of SNR is shown in Table 2. For the periodogram method, the results were divided into two categories: estimation with maximum magnitude and estimation center-of-mass method. The recorded data are presented in relative percentage values to present the obvious level of accuracy for values of mean frequencies. Table 2 indicates that using a suitable method is important for certain performance criteria. For average bias, the periodogram method used with maximum magnitude produces the lowest bias. For variation in estimate and RMSE, the periodogram with center-of-mass and AR method produced the best result. As far as statistical accuracy criteria are concerned, it is difficult to conclude which estimators provide the best performance since each method has their strength.

Again, it is worth noting that for  $f_m=0.3$  kHz, The AR method was only successful if the spectra were computed with model orders  $p=15$  or using lower frequency resolution. As for AR spectra for  $f_m=2.1$  kHz and 4 kHz, the spectral estimates with a single peak were possible with  $p<4$ . This indicates that the AR method is guaranteed not to work for lower orders. Nonetheless, for a practical SoG radar system, this is not a major limitation since the many modern microprocessors are equipped with sufficient computational capabilities to support AR computation with high model order. The performance trends of each method as a function of Doppler frequency are shown in Figures 6(a) to (c). Although the estimated data fluctuate across the Doppler frequencies, we observed trends and we visualized the trend by using the linear regression model. The solid lines with markers correspond to the SNR values.

Table 2. Mean frequency estimation using maximum magnitude.

SNR (dB)	$\hat{f}_m$ (kHz)	Periodogram and Maximum Magnitude			Periodogram and Mass Centre			Autoregressive and Maximum Magnitude		
		Rel. Bias (%)	Rel. $\sigma_0$ (%)	Rel. RMSE (%)	Rel. Bias (%)	Rel. $\sigma_0$ (%)	Rel. RMSE (%)	Rel. Bias (%)	Rel. $\sigma_0$ (%)	Rel. RMSE (%)
50	0.3	0.3	7.1	7.1	1.3	3.2	3.4	2.2	1.3	2.6
	2.1	0.2	6.1	6.1	1.1	2.5	2.7	2.8	1.4	3.1
	4.0	0.0	6.1	6.1	0.8	2.2	2.3	2.7	1.0	2.8
40	0.3	0.4	7.1	7.1	1.3	3.2	3.4	1.2	1.3	1.8
	2.1	0.2	6.1	6.1	1.1	2.5	2.7	1.3	1.3	1.8
	4.0	0.0	6.1	6.1	0.8	2.2	2.3	2.5	1.0	2.7
30	0.3	0.8	6.9	6.9	1.2	2.8	3.0	1.1	1.3	1.7
	2.1	0.6	6.5	6.5	1.6	2.9	3.3	3.0	1.5	3.3
	4.0	0.5	6.7	6.7	0.4	2.0	2.1	1.1	1.0	1.5
20	0.3	0.4	7.5	7.5	1.2	3.3	3.5	8.4	2.4	8.7
	2.1	0.4	5.5	5.5	1.4	2.3	2.7	8.3	1.9	8.5
	4.0	0.5	7.1	7.2	0.6	2.2	2.3	1.0	1.1	1.4

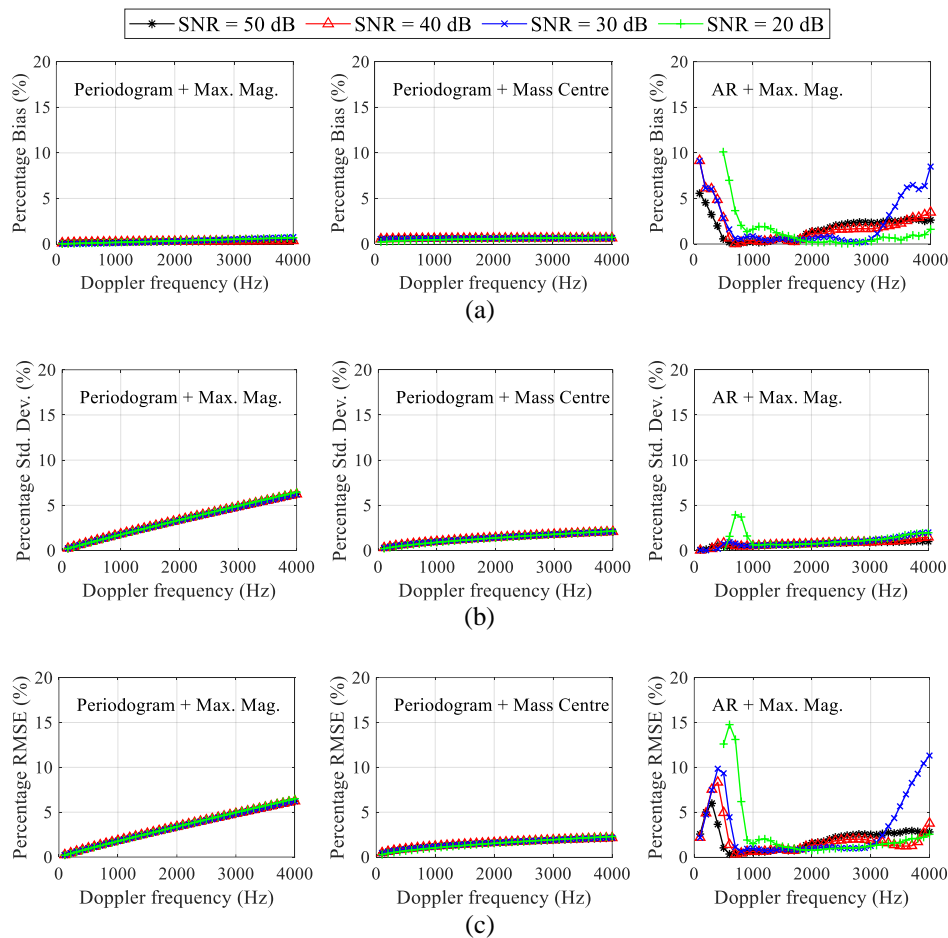


Figure 6. The trend of relative percentage (a) bias, (b) standard deviation, and (c) RMSE of the spectral estimation methods



The estimated percentage of bias as a function of Doppler frequency is shown in Figure 6(a). The periodograms methods show the same linear trend which is apparent in both figures. There is a small increase in bias towards high Doppler frequency, but the increase is not appreciable. On the other hand, the AR method performance is somewhat non-linear, and they tend to have appreciable variation between SNR values. The AR method estimates were only relatively flat for Doppler frequency between the range of 1 kHz and 3 kHz but increased bias outside of the region, suggesting that model order may not be optimal. Subsequently, the estimated percentage of standard deviation as a function of Doppler frequency is shown in Figure 6(b). All estimates show an approximately linear trend, but between the two methods, the AR method shows the lowest increase in standard deviation with increasing Doppler frequency. Expectedly, the periodogram with maximum magnitude exhibited the largest variance in estimates. The estimated percentage of RMSE as a function of Doppler frequency is shown in Figure 6(c). Evidently, the increase in RMSE is accompanied by an increase in standard deviation. The periodogram method with center-of-mass method performs well indicated with the linear trend but with a small slope. As with the AR method, this method only shows a good prediction for mean Doppler frequency between 1 kHz and 3 kHz but deviated appreciably outside of this region.

#### 4. CONCLUSION

This work compares two common spectral estimation methods namely Fourier transform based on periodogram, and AR method based on Burg algorithm to determine the mean frequency of Doppler signal found in SoG radar systems. A total of 80,000 artificial Doppler signals were generated and used as a test signal. The methods' performance was evaluated based on their measurement bias, standard deviation, and RMSE. The periodogram method is an effective method that can be applied to the time-domain Doppler signal even in the presence of considerable noise (20 dB). With the combination of mass-center detection method, the periodogram method can be said to provide good accuracy with consistent performance in the three criteria tested. Furthermore, this method is relatively simpler to use than the AR method. It can be deduced that, although the AR Burg method is theoretically superior in terms of resolution. It offered no significant advantages here. The AR method demonstrated only a slight advantage on RMSE when compared to the periodogram with center-of-mass method and was only appreciable within a narrow bandwidth of Doppler frequencies between 0.8 kHz and 1.3 kHz. Within this region, the AR method performs the best. Some factors such as the ratio of Doppler spectrum bandwidth to the sampling frequency might have a profound influence on the overall performance. The fact that fixing AR model order to a fixed value here seems to be a bad choice because they did not generate high consistency in the trends of the performance. This gives the impression that higher model order is desirable to better approximate the spectrum and thus, enhancing the performance of estimates. However, this study is not discussed here.

#### ACKNOWLEDGEMENTS

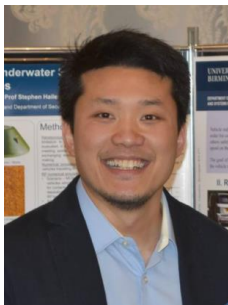
This research is fully supported by MITRANS grant, 600-RMC/MITRANS\_IRES 5/3(003/2020). The authors would like to thank Research Management Institute (RMI) and Universiti Teknologi MARA for all the supports.




#### REFERENCES

- [1] T. Reissland, B. Lenhart, J. Lichtblau, M. Sporer, R. Weigel, and A. Koelpin, "Robust correlation based true-speed-over-ground measurement system employing a FMCW radar," in *2018 15th European Radar Conference (EuRAD)*, Sep. 2018, pp. 87–90, doi: 10.23919/EuRAD.2018.8546663.
- [2] E. Klinefelter and J. A. Nanzer, "Millimeter-wave interferometric radar for speed-over-ground estimation," in *2020 IEEE/MTT-S International Microwave Symposium (IMS)*, Aug. 2020, pp. 1023–1026, doi: 10.1109/IMS30576.2020.9224063.
- [3] F. Michler, B. Scheiner, T. Reissland, R. Weigel, and A. Koelpin, "Micrometer sensing with microwaves: precise radar systems for innovative measurement applications," *IEEE Journal of Microwaves*, vol. 1, no. 1, pp. 202–217, Jan. 2021, doi: 10.1109/JMW.2020.3034988.
- [4] D. V. Khablov, "Autonomous navigation system of ground transport based on Doppler sensors for measuring vector velocity," *Measurement Techniques*, vol. 61, no. 4, pp. 384–389, Jul. 2018, doi: 10.1007/s11018-018-1438-x.
- [5] C. K. Song, M. Uchanski, and J. K. Hedrick, "Vehicle speed estimation using accelerometer and wheel speed measurements," SAE International, Warrendale, PA, Jul. 2002. doi: 10.4271/2002-01-2229.
- [6] J. Crestel, B. Emile, M. Guillon, and D. Menard, "A Doppler frequency estimate using the instantaneous frequency," in *Proc. 13th International Conference on Digital Signal Processing*, 1997, vol. 2, pp. 777–780, doi: 10.1109/ICDSP.1997.628467.
- [7] J. Crestel, M. Guillon, and H. Chuberre, "An enhanced method for the estimation of a Doppler frequency," in *European Signal Processing Conference, 1996. EUSIPCO 1996. 8th*, 1996, pp. 1–4.
- [8] W. Kleinhempel, D. Bergmann, and W. Stammer, "Speed measure of vehicles with on-board Doppler radar," in *92 International Conference on Radar*, 1992, pp. 284–287.
- [9] J. Dybedal, "Doppler radar speed measurement based on A 24 GHz radar sensor," Thesis, Institutt for elektronikk og




- telekomunikasi, 2013.
- [10] S. Yoshida, S. Izumi, K. Kajihara, Y. Yano, H. Kawaguchi, and M. Yoshimoto, "Energy-efficient spectral analysis method using autoregressive model-based approach for internet of things," *IEEE Transactions on Circuits and Systems I: Regular Papers*, vol. 66, no. 10, pp. 3896–3905, Oct. 2019, doi: 10.1109/TCSL.2019.2922990.
  - [11] R. Schubert, P. Heide, and V. Mágori, "Microwave Doppler sensors measuring vehicle speed and travelled distance: realistic system tests in railroad environment," *Proc. MIOP'95 Microw. & Optronics C.*, 1995.
  - [12] P. Zetterlund, "Measuring traveled distance using doppler radar sensors,," Master Thesis, Linköping University, 2004.
  - [13] T. M. Hyltin, T. D. Fuchser, H. B. Tyson, and W. R. Regueiro, "Vehicular radar speedometer," SAE International, Warrendale, PA, Feb. 1973. doi: 10.4271/730125.
  - [14] E. Klinefelter and J. A. Nanzer, "Interferometric microwave radar with a feedforward neural network for vehicle speed-over-ground estimation," *IEEE Microwave and Wireless Components Letters*, vol. 30, no. 3, pp. 304–307, Mar. 2020, doi: 10.1109/LMWC.2020.2966191.
  - [15] D. S. Zrnić, "Simulation of weatherlike Doppler spectra and signals," *Journal of Applied Meteorology*, vol. 14, no. 4, pp. 619–620, Jun. 1975, doi: 10.1175/1520-0450(1975)014<0619:SOWDSA>2.0.CO;2.
  - [16] K. K. M. Shariff, E. Hoare, L. Daniel, M. Antoniou, and M. Cherniakov, "Comparison of adaptive spectral estimation for vehicle speed measurement with radar sensors," *Sensors*, vol. 17, no. 4, Apr. 2017, doi: 10.3390/s17040751.
  - [17] J. G. Proakis and D. K. Manolakis, *Digital signal processing*, 4 edition. Upper Saddle River, N.J: Pearson, 2006.
  - [18] A. Schlögl, "A comparison of multivariate autoregressive estimators," *Signal Processing*, vol. 86, no. 9, pp. 2426–2429, Sep. 2006, doi: 10.1016/j.sigpro.2005.11.007.
  - [19] P. M. T. Broersen, "Finite sample criteria for autoregressive order selection," *IEEE Transactions on Signal Processing*, vol. 48, no. 12, pp. 3550–3558, 2000, doi: 10.1109/78.887047.
  - [20] R. Palaniappan, "Towards optimal model order selection for autoregressive spectral analysis of mental tasks using genetic algorithm," *International Journal of Computer Science and Network Security*, vol. 6, no. 1A, pp. 153–162, 2006.
  - [21] P. Ahrendt, "Music genre classification systems-a computational approach," *Informatics and Mathematical Modelling*, 2006.
  - [22] T. S. Rao, S. S. Rao, and C. R. Rao, *Time series analysis: methods and applications*. Elsevier, 2012.
  - [23] F. Castanié, *Spectral analysis: parametric and non-parametric digital methods*. Wiley, 2006.
  - [24] B. Boashash, "Estimating and interpreting the instantaneous frequency of a signal. II. Algorithms and applications," *Proceedings of the IEEE*, vol. 80, no. 4, pp. 540–568, Apr. 1992, doi: 10.1109/5.135378.
  - [25] T. Meyer, "Root mean square error compared to, and contrasted with, standard deviation," *Surveying and Land Information Science*, vol. 72, no. 3, pp. 107–108, 2012.

## BIOGRAPHIES OF AUTHORS






**Khairul Khaizi Mohd Shariff**    received his B.Eng. in electronics in Universiti Teknologi MARA in 2003. M.Sc. in Communications and Computer in 2011 from Universiti Kebangsaan Malaysia and PhD in Electronics from University of Birmingham, United Kingdom in 2019. He is currently working as a lecturer in Universiti Teknologi MARA and serves as a researcher in the Microwave Research Institute in the same university. His main area of studies is speed-over-ground radar and radar signal processing. He can be contacted at email: khairul Khaizi@uitm.edu.my.






**Suraya Zainuddin**    is a lecturer in Faculty of Electrical and Electronic Engineering Technology (FTKEE), Universiti Teknikal Malaysia Melaka (UTeM). She received the Bachelor of Engineering (Electrical-Telecommunication) from Universiti Teknologi Malaysia (UTM) in 2003, M.Sc. in Telecommunication and Information Engineering in from Universiti Teknologi MARA (UiTM) in 2015 and PhD in Electrical Engineering from the similar university in 2020. Her main research areas involved the studies in Multiple-input multiple-output (MIMO) radar, radar system and application, signal processing and radar detection. She can be contacted at email: suraya@utem.edu.my.






**Noor Hafizah Abdul Aziz**    received her B.Eng. in microelectronic engineering and M.Sc. in electrical, electronic and system engineering from the Universiti Kebangsaan Malaysia, Selangor in 2004 and 2007, respectively. Subsequently, her PhD in Wireless Communications Engineering from the Universiti Putra Malaysia, Selangor in 2018. Since 2008, she has been with the Centre for Communication Engineering Studies, Faculty of Electrical Engineering, Universiti Teknologi MARA, Malaysia, where she is currently works as a senior lecturer. She is undertaking her research on passive forward scattering radar system, classification, signal processing and applications of communication system. She can be contacted at email: noor4083@uitm.edu.my.



**Nur Emileen Abd Rashid**    is currently a Senior Lecturer at University Technology MARA. She obtained the Bachelor of Electrical Engineering (Telecommunication Engineering) from the Universiti Kebangsaan Malaysia in 2001 and subsequently her M.Sc. in Computer, Communication and Human Centered Engineering from the University of Birmingham, UK in 2002. She pursued her studies and received her PhD in 2011 from the same university. She has contributed much of her expertise in areas related Radar Technology, Telecommunication signal processing and clutter modelling. Dr. Nur Emileen is an active member of IET, IEEE and MyRAN. She can be contacted at email: emileen98@uitm.edu.my.



**Nor Ayu Zalina Zakaria**    is currently a Senior Lecturer in School of Electrical Engineering, College of Engineering, University Teknologi MARA, Malaysia and has almost 18 years working experience in an engineering education. She obtained her PhD degree in Radar Technology from University of Birmingham, United Kingdom in 2017. She received her BEng (Hons) in Electronics and Telecommunication Engineering from University Malaysia Sarawak and Master in Mobile and Satellite Communication Engineering from University of Surrey, United Kingdom in 2000 and 2003 respectively. Her areas of interest mainly in radar technology particularly, radar detection and related work in clutter analysis for forward scatter radar. She can be contacted at email: norayu713@uitm.edu.my.